J. Fluid Mech. (1995), *vol.* 284, *pp.* 341–358

Bifurcations and nonlinear dynamics of surface waves in Faraday resonance

By H. FRIEDEL, E. W. LAEDKE AND K. H. SPATSCHEK

Institut für Theoretische Physik I, Heinrich-Heine-Universität Düsseldorf, D-40225 Düsseldorf, Germany

(Received 12 April 1994 and in revised form 7 September 1994)

The nonlinear dynamics of nonlinear modulated cross-waves of resonant frequency ω_1 and carrier frequency $\omega \approx \omega_1$ is investigated. In a long channel of width b, that contains fluid of depth d and which is subjected to a vertical oscillation of frequency 2ω, the wave can appear in solitary form. As has been shown previously, the solitary wave is only stable in a certain parameter regime; depending on damping and driving amplitudes the wave becomes unstable. The nonlinear development of the instabilities of solitary waves is the central problem of this paper. It is shown how instabilities are saturated following generic routes to chaos in time with spatially coherent structures. Finally, the case of time-modulated driving amplitudes is also considered. In most cases it appears that nonlinear waves of simple spatial structures take part in the nonlinear dynamics, but a few cases of spatial chaos are also reported.

1. Introduction

The experimental observation of a non-propagating hydrodynamic soliton by Wu, Keolian & Rudnick (1984) opened the wide field of the existence and dynamics of resonantly excited solitary water waves. The basic theory of this phenomenon was developed by Miles (1984 *a, b*) and Larraza & Putterman (1984). Meanwhile we have beautiful experiments (e.g. Funakoshi & Inoue 1987, 1990, 1992; Ezerskii *et al.* 1986; Ciliberto & Gollub 1985; Simonelli & Gollub 1989; Denardo *et al.* 1990; Guthart & Wu 1991; Wei *et al.* 1990; Chen & Wei 1994) and numerical simulations (e.g. Umeki 1991 *a, b*; Kambe & Umeki 1990) which show that this area is rapidly growing and extremely interesting. Nonlinear surface waves can act as a paradigm for classical nonlinear dynamics in systems with an infinite number of degrees of freedom.

In a series of experiments Funakoshi & Inoue (1987, 1990, 1992, and references therein) found existence regions for resonantly excited nonlinear waves using cylindrical geometry. They also investigated the instabilities and possible routes to chaos, thereby clarifying by clear experiments several theoretical predictions. Ezerskii *et al.* (1986) did experiments on parametric excitation of a capillary ripple on a silicone surface, observing in space two-dimensionally chaotic states. Ciliberto & Gollub (1985) as well as Simonelli & Gollub (1989) studied mode coupling in Faraday resonance. Wei *et al.* (1990) and Chen & Wei (1994) made detailed experimental studies of non-propagating solitons and their transition to chaos as well as an investigation on the effects of periodically modulated drivers. We also refer the reader to recent overviews which can be found in Guthart & Wu (1991) and Miles & Henderson (1990).

The theoretical description of a nonlinear modulated cross-wave starts from the model equation (Miles 1984 *b*)

$$\mathrm{i}(r_t + \alpha r) + Br_{xx} + \left(\beta + A|r|^2\right) r + \gamma r^* = 0 \tag{1.1}$$

for the complex amplitude r of the dominant cross-wave. Here, α is the linear damping ($\alpha > 0$), and the terms βr and γr^* (with $\gamma > 0$, but β can have both signs) appear because of vertical oscillations $z = a_0 \cos(2\omega t)$ at approximately twice the carrier frequency $\omega \approx \omega_1 = (gk \tanh kd)^{1/2}$. The other parameters, $B > 0$ and A (for the modulationally unstable case $A > 0$; in general, A can have both signs, but here we consider only the modulationally unstable situation which results in soliton formation) can be scaled out, so that with

$$\lambda := -\beta - \mathrm{i}\alpha \tag{1.2}$$

and

$$\delta := \gamma \rightarrow \delta(t) \equiv \delta\,(1 + a_m \sin \Omega t)\ , \tag{1.3}$$

we can write (1.1) in the standard form

$$\mathrm{i}\psi_t + \psi_{xx} + |\psi|^2\psi - \lambda_r\psi - \mathrm{i}\lambda_i\psi + \delta(t)\psi^* = 0\,. \tag{1.4}$$

By allowing $\delta(t)$ to be a function of time t ($|a_m| < 1$) we are able to include a slow modulation of the oscillation amplitude (Chen & Wei 1994). But first, by putting $a_m \equiv 0$, we restrict ourselves to the original Miles model. Note that recently (1.1) was generalized for solutions without compact support (Sasaki 1993; Miles 1994).

In 1991 several papers appeared which discussed the stability of stationary solutions. Two investigations (Laedke & Spatschek 1991; Barashenkov, Bogdan & Korobov 1991) concentrated on the (localized) solitary wave solution

$$G = (2(\lambda_r - \delta\cos 2\varphi))^{1/2}\,\mathrm{sech}\left[(\lambda_r - \delta\cos 2\varphi)^{1/2}\,(x - x_0)\right] \tag{1.5}$$

where the phase φ in $\psi \equiv G\mathrm{e}^{\mathrm{i}\varphi}$ is determined by the algebraic relation

$$\lambda_i + \delta \sin 2\varphi = 0\,. \tag{1.6}$$

The relation (1.6) suggests an existence condition of the form

$$\delta > -\lambda_i \tag{1.7}$$

for non-trivial solutions. Note that then (1.6) has two solutions which we denote by the index $\pm$.

Solutions (on a finite domain) with periodicity length L were also investigated (but preferentially numerically). Besides vanishing boundary conditions at infinity, boundary conditions at finite distance are of especial interest, because of direct applicability to the experiments. The theoretical understanding of the rich dynamics inherent in the Miles equation was much advanced by Umeki (1991 *a, b*) and Kambe & Umeki (1990). By numerical simulations in finite systems with periodic boundary conditions they obtained noidal wave solutions and, in the time-dependent case they found periodic, quasi-periodic, and chaotic motions where – in most cases – the spatially coherent noidal waves played the dominant role.

In this paper we shall mainly concentrate on the solitary wave solution since we believe that – compared with the progress obtained by Umeki and Kambe for the finite-dimensional case – some work is still necessary to understand the basic dynamics of the solitary wave solutions. The solitary wave case has – compared with

the noidal wave case – the advantage that some analytical results can be obtained in simpler form. It turns out that the principal features are similar to those on the infinite domain. As we shall show below, the *c*-noidal and *d*-noidal waves exist as counterparts of the soliton solution (1.5).

Since we have a quite clear picture of the existence and instabilities of nonlinear solitary solutions, the problem of predicting and understanding the nonlinear developments becomes of major interest. This paper is devoted to this new aspect; it is organized as follows. First, in § 2, we present an overview of the existence and stability properties. Phenomenologically known results are supported by analytical arguments. Then, in § 3 we discuss the various scenarios of nonlinear developments, depending on the paths in parameter space. We shall pick out one route (see § 3.1) in more detail in order to support the numerical findings by analytic theory. In § 4 we briefly report on some phenomena for modulated driving amplitudes. The paper is concluded by a short summary and outlook.

2. Existence and stability results

2.1. *Existence of non-trivial solutions*

Let us consider a system of length L with $x_1 \leqslant x \leqslant x_2$ and $x_2 - x_1 = L$. (Later we can also go to $L \to \infty$.) Defining

$$N_0^2 := \int_{x_1}^{x_2} |\psi|^2 \mathrm{d}x \tag{2.1}$$

and

$$N_1^2 = \int_{x_1}^{x_2} |\partial_x \psi|^2 \mathrm{d}x \tag{2.2}$$

one can prove

$$|\psi(x)|^2 \leqslant 2N_0 N_1 + L^{-1} N_0^2 \tag{2.3}$$

and

$$N_0^2 \leqslant C \mathrm{e}^{2(\lambda_i + \delta)t}\,, \tag{2.4}$$

where C is a constant. Thus, when $\delta < -\lambda_i$ we find $N_0 \to 0$ for $t \to \infty$.

To prove (2.3) and (2.4) we start with the identity

$$|\psi(x)|^2 = \int_{\xi}^{x} \frac{\partial |\psi(x')|^2}{\partial x'} \mathrm{d}x' + |\psi(\xi)|^2\,, \tag{2.5}$$

where $\xi, x \in [x_1, x_2]$. Using $|(\partial_x \psi)\psi^*| \leqslant |\partial_x \psi||\psi|$ and $|x - \xi| \leqslant |x_2 - x_1|$ we obtain by the Cauchy–Schwarz inequality and the mean value theorem of analysis

$$|\psi(x)|^2 \leqslant 2 \left(\int_{x_1}^{x_2} |\partial_x \psi|^2 \mathrm{d}x \right)^{1/2} \left(\int_{x_1}^{x_2} |\psi|^2 \mathrm{d}x \right)^{1/2} + \frac{1}{L} \int_{x_1}^{x_2} |\psi|^2 \mathrm{d}x\,. \tag{2.6}$$

This is identical with (2.3).

For (2.4) we differentiate N_0^2 with respect to t and make use of the dynamic equation for ψ. A short calculation leads to

$$\frac{\mathrm{d}N_0^2}{\mathrm{d}t} = 2\lambda_i N_0^2 + \mathrm{i}\delta \int_{x_1}^{x_2} \left(\psi^{*2} - \psi^2 \right) \mathrm{d}x\,. \tag{2.7}$$

Periodic boundary conditions have been used. Note that in our calculation δ can even

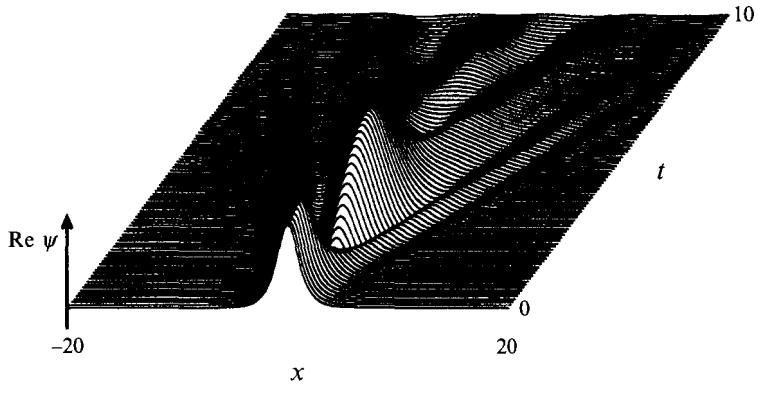

FIGURE 1. Starting with a solitary wave solution for $\lambda_r = 1, \lambda_i = -0.5, \delta = 0.4$, the solution is being damped out with increasing time.

be periodically modulated, e.g. we choose the modulation $a_m \sin \Omega t$ as shown by (1.3) in this presentation. Using the triangle inequality ($\psi := a + \mathrm{i}b$, $\mathrm{i}(\psi^{*2} - \psi^2) = 4ab \leqslant 2(a^2 + b^2) = 2\psi^*\psi$) we can transform (2.7) into

$$\frac{\mathrm{d}N_0^2}{\mathrm{d}t} \leqslant 2(\lambda_i + |\delta|) N_0^2 . \tag{2.8}$$

From here (2.4) follows immediately.

However to conclude from (2.3) and (2.4) that under this condition only the trivial solution exists, we have to analyse the dynamics of N_1. One can show that N_1 obeys

$$(N_1 - N_0^3)^2 \leqslant E_s + N_0^6 + L^{-1}N_0^4 - \lambda_r N_0^2 + \delta N_0^2 , \tag{2.9}$$

which proves that N_1 is bounded for $N_0 \to 0$; E_s is a constant. Thus from (2.3) we can conclude that $\psi \to 0$ for $\delta < -\lambda_i$. Figure 1 demonstrates such a behaviour for a typical choice of parameters. When starting with any initial value distribution (e.g. a solitary one) in the parameter region $\delta < -\lambda_i$, the solution tends to zero. Physically this behaviour is understandable, since we have a balance between driving (δ) and damping ($-\lambda_i$). If the latter is too strong, the solution dies out. To prove (2.9) we first define the energy

$$E := -\int_{x_1}^{x_2} \left\{ \tfrac{1}{2}|\psi|^4 - |\partial_x \psi|^2 - \lambda_r |\psi|^2 + \delta(\psi^{*2} + \psi^2) \right\} \mathrm{d}x . \tag{2.10}$$

Using the dynamic equation for ψ as well as the inequality (2.3) we obtain after some algebra for the time-variation of E

$$\frac{\mathrm{d}E}{\mathrm{d}t} \leqslant 2\lambda_i \left[(N_1 - N_0^3)^2 - N_0^6 - \frac{1}{L}N_0^4 - \lambda_r N_0^2 + \frac{\delta}{2}\int_{x_1}^{x_2} (\psi^2 + \psi^{*2})\,\mathrm{d}x \right] - \frac{\dot{\delta}}{2}\int_{x_1}^{x_2} (\psi^2 + \psi^{*2})\,\mathrm{d}x , \tag{2.11}$$

which can be simplified to

$$\frac{\mathrm{d}E}{\mathrm{d}t} \leqslant -2\lambda_i \left[N_0^6 + \frac{1}{L}N_0^4 - \lambda_r N_0^2 + \delta(1 + a_m) N_0^2 \right] + \delta a_m \Omega N_0^2 . \tag{2.12}$$

Thus E is bounded when N_0 tends to zero for $\delta < -\lambda_i$. We designate this bound by

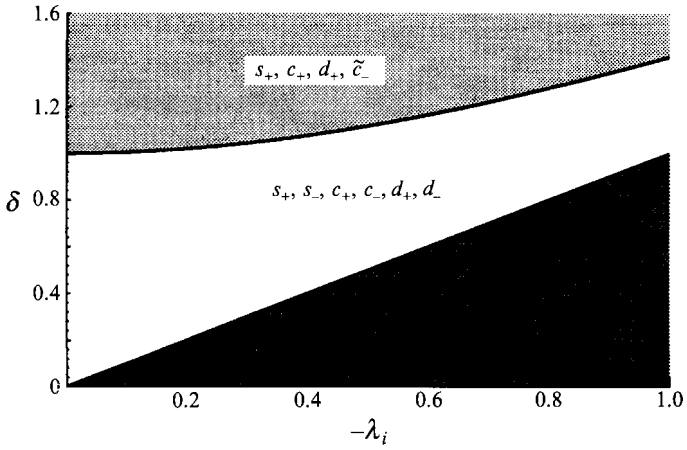

FIGURE 2. Existence diagram for the solutions (2.14)–(2.17) in the case $\lambda_r = +1$. Note that below the line $\delta = -\lambda_i$ no solutions exist whereas the others only exist in the marked areas.

E_s. Going back to the definition of E, i.e. (2.10), and making use of the inequality (2.3), we immediately arrive at (2.9).

2.2. *Classes of stationary solutions*

Besides the constraint $\delta > -\lambda_i$ the *localized* solution (1.5) requires $\lambda_r - \delta\cos 2\varphi > 0$. For given λ_i and δ equation (1.6) determines (two solutions of) φ (with index $\pm$). The extra condition $\lambda_r - \delta\cos 2\varphi > 0$ originates from the localization condition ($|\psi| \to 0$ for $|x| \to \infty$). However, since we have a finite system, the solution (1.5) is only a special one. In general, we should look for solutions of

$$\frac{1}{2}\left(\frac{\mathrm{d}G}{\mathrm{d}x}\right)^2 + \tfrac{1}{4}G^4 - \tfrac{1}{2}(\lambda_r - \delta\cos 2\varphi)\,G^2 = c\,, \tag{2.13}$$

where c is a constant of integration ($c = 0$ for localized solutions on the infinite domain). From here it becomes clear that $\lambda_r - \delta\cos 2\varphi > 0$ is only necessary for decaying (at $|x| \to \infty$) solutions, but not for solutions on the finite domain. The noidal wave solutions can be found in a paper by Umeki (1991 *a*). But note that for stationary solutions without compact support a shift in the resonance frequency has to be taken into account (Sasaki 1993; Miles 1994). Let us summarize here the existence diagrams of constant-phase solutions for $\lambda_r > 0$ and $\lambda_r < 0$ separately. (Without loss of generality we put $|\lambda_r| = 1$.)

Let us introduce the abbreviations

$$s_\pm = \sqrt{2}\eta_\pm \operatorname{sech}[\eta_\pm(x - x_0)]\,,\{\text{ infinite domain }\}\,, \tag{2.14}$$

$$c_\pm = \left(\frac{2k^2}{k^2 - k'^2}\right)^{1/2} \eta_\pm \operatorname{cn}\left[\left(\frac{1}{k^2 - k'^2}\right)^{1/2} \eta_\pm(x - x_0)\right]\,, \tag{2.15}$$

$$d_\pm = \left(\frac{2}{1 + k'^2}\right)^{1/2} \eta_\pm \operatorname{dn}\left[\left(\frac{1}{1 + k'^2}\right)^{1/2} \eta_\pm(x - x_0)\right]\,, \tag{2.16}$$

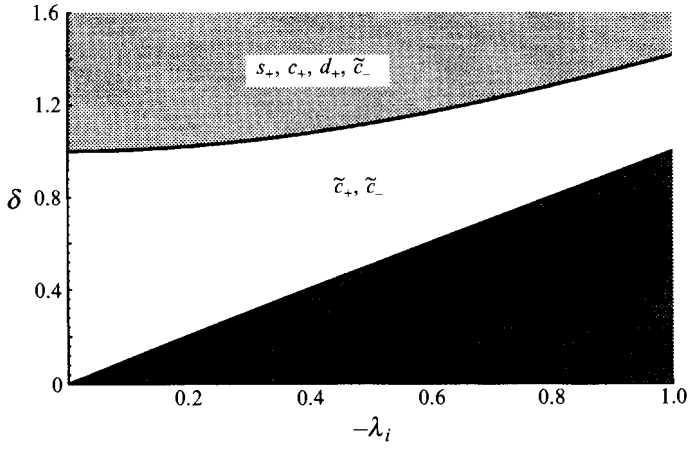

FIGURE 3. Existence diagram for the solutions (2.14)–(2.17) in the case $\lambda_r = -1$. Note that below the line $\delta = -\lambda_i$ no solutions exist whereas the others only exist in the marked areas.

$$\tilde{c}_\pm = \left(\frac{2k^2}{k'^2 - k^2}\right)^{1/2} \tilde{\eta}_\pm \operatorname{cn}\left[\left(\frac{1}{k'^2 - k^2}\right)^{1/2} \tilde{\eta}_\pm (x - x_0)\right], \tag{2.17}$$

for $\eta_\pm^2 = \lambda_r - \delta\cos 2\varphi_\pm > 0$ or $\tilde{\eta}_\pm^2 = -\lambda_r + \delta\cos 2\varphi_\pm > 0$, respectively. With finite periodicity length, the noidal solutions appear with modulus k ; k' follows from η, L, and k by a relation involving a complete elliptical integral $K(k)$. However not all solutions (2.14)–(2.17) exist for all parameter values. Depending on the sign of λ_r we have two different scenarios, depicted in figures 2 and 3, respectively.

2.3. *Stability diagram*

In the following we summarize the known stability results for the solitary wave $G = s_\pm$. First, it was shown by Laedke & Spatschek (1991) as well as Barashenkov *et al.* (1991) that s_- is always unstable. Furthermore, Laedke & Spatschek (1991) showed that s_+ becomes unstable for $\delta > (\lambda_r^2 + \lambda_i^2)^{1/2}$. The stability of the soliton in the region $-\lambda_i < \delta < (\lambda_r^2 + \lambda_i^2)^{1/2}$ is not easy to discuss. Laedke & Spatschek (1991) used a perturbative scheme to demonstrate that the soliton is stable just above the line $\delta = -\lambda_i$. On the other hand, Barashenkov *et al.* (1991) were able to demonstrate that below the curve $\delta = (\lambda_r^2 + \lambda_i^2)^{1/2}$ in some region an oscillatory instability already exists. The by now quite complete understanding of the stability behaviour of the soliton solution s_+ is summarized in figure 4. For $\lambda_r = +1$ we have shown the stable region I of an existing stationary soliton solution. The instability from I $\rightarrow$ III was discussed by Laedke & Spatschek (1991), whereas the stabiltiy border I $\rightarrow$ II was detected by Barashenkov *et al.* (1991).

In 1991 Umeki discussed parts of the behaviour of solutions with periodic boundary conditions ($L \approx 15.5$). He calculated constant-phase stationary states, which are zero, uniform, and noidal solutions denoted $c_\pm$ and $d_\pm$. Umeki also obtained a perturbative solution near the uniform state with non-constant phase. He found a good agreement of this perturbative state with numerically integrated solutions of the stationary system.

The stability of the quiescent and uniform states was discussed by Umeki (1991), where it turned out that there are co-dimension-2 bifurcation points. At these points

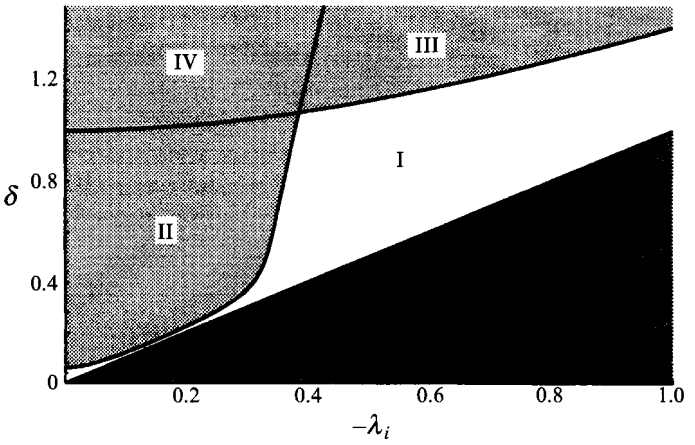

FIGURE 4. Stability diagram for the soliton solution s_+ in the case $\lambda_r = +1$. Only in the completely blank region I does the soliton exist in a stable form.

Umeki derived amplitude equations for perturbative mixed-mode stationary states of the form

$$\Psi = (p + iq) = (p_1 + iq_1)\cos(k_1 x) + (p_2 + iq_2)\cos(k_2 x) \tag{2.18}$$

with $k_2 = mk_1$, m being positive integer.

For the non-uniform stationary solutions the linear eigenvalue problem was solved numerically by expanding the perturbation into a Fourier series and truncating higher-order terms. This analysis showed that there are Hopf and pitchfork bifurcations in the bifurcation curves for both *cn*- and *dn*-type solutions. So far, the stability diagrams for noidal-wave-like solutions do not exist in forms similar to figure 4 for the soliton, but after the work of Umeki (1991 *a*) there is no doubt that they could be produced in full detail if it turns out that they are needed. However, when considering envelopes without compact support (Sasaki 1993; Miles 1994) a modification of (1.1) should be taken into account. In this paper we shall mainly concentrate on localized solutions in sufficiently large systems (of not too small depths) such that for the following conclusions the additional (to (1.1)) mass conserving term is not important.

3. Nonlinear developments of the soliton instabilities

Starting with a solitary wave solution in the stable regime I of figure 4, we can change parameters leaving the stability zone I. Various generic paths are possible. The first – quite trivial one – is to penetrate below the curve $\delta = -\lambda_i$ in the $(\delta, -\lambda_i)$-parameter space. The result has already been discussed in § 2.1; the space-dependent solutions die out because of too strong damping. The other paths will now be discussed in more detail, and most emphasis is on the I → II transition.

3.1. *The transition I → III*

Any numerical simulation starts with a finite system. Thus, when studying numerically the nonlinear development of an unstable solution s_+ in region III, we actually take c_+ (with Dirichlet boundary conditions) or d_+ (with von Neumann boundary conditions) for a large system ($L \to \infty$). Actually, both the boundary conditions just mentioned are special forms of periodic boundary conditions. However, for the dynamics it

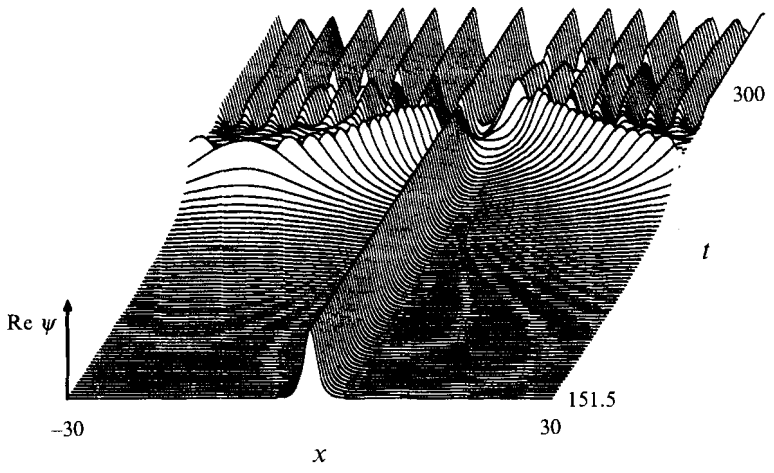

FIGURE 5. Time development of an unstable soliton solution in the region III of figure 4. Here we have chosen $\lambda_r = 1, \lambda_i = -1$, and $\delta = 1.45$.

makes a big difference whether one investigates long or small systems, as we shall show below. It is interesting to follow the previously published (Laedke & Spatschek 1991) linearly unstable mode into the nonlinear regime. A saturation of instability is shown in figure 5. The result reported there is typical, i.e. we always end up with c-noidal, d-noidal solutions, or a weak time-dependent mixture of both. Thus the transition I $\rightarrow$ III is a bifurcation in space without additional generic nonlinear behaviour in time. It is important to analyse such a behaviour in more mathematical detail; the analytical calculations will be presented in a separate paper.

3.2. *The transition I $\rightarrow$ II*

As has been noted already by Barashenkov *et al.* (1991), at the border line between regions I and II a Hopf bifurcation takes place, i.e. we have an oscillatory instability. By numerical computations we find that the new state, close to the onset of instability, is an oscillating soliton as depicted in figure 6. In the Appendix we present a theory for the nonlinearly saturated state. The Newell–Whitehead (1969) procedure is used there to derive for the amplitude A of the unstable mode a nonlinear equation of the form

$$A_{t_2} = \alpha A + \beta A_{x_1 x_1} + \gamma |A|^2 A \,. \tag{3.1}$$

As can be seen from the Appendix, t_2 and x_1 designate the weak time- and space-dependencies of the amplitude A, respectively. The coefficients α and γ have been calculated numerically. One can show that (close to the onset of instability) the new state is stable, and the analytically calculated saturation amplitude agrees very well with the numerical simulations. Figure 7 depicts the maximum elongation $\Delta\psi_{\max}$ above the stationary solitary wave amplitude as a function of the deviation from the onset of instability. There is a good agreement between our analytical predictions and the numerical simulation.

However, further decreasing $-\lambda_i$ (e.g. for fixed δ) shows that the oscillating soliton becomes unstable, and a period-doubling route to temporal chaos appears. We can view this behaviour in various ways. Figure 8 shows plots of $\mathrm{Im}\,\psi(x = 0)$ *vs.* $\mathrm{Re}\,\psi(x = 0)$ for different values of λ_i (keeping δ fixed). Figure 9 presents the corresponding Feigenbaum diagram. Using diagnostic techniques known from low-

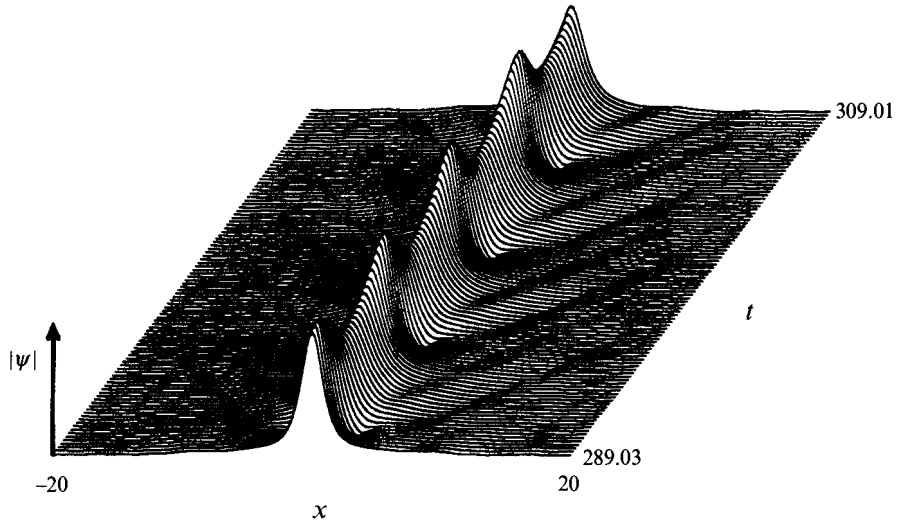

FIGURE 6. Space–time plot of an 'oscillating soliton' for $\lambda_r = 1, \lambda_i = -0.29$, and $\delta = 0.4$.

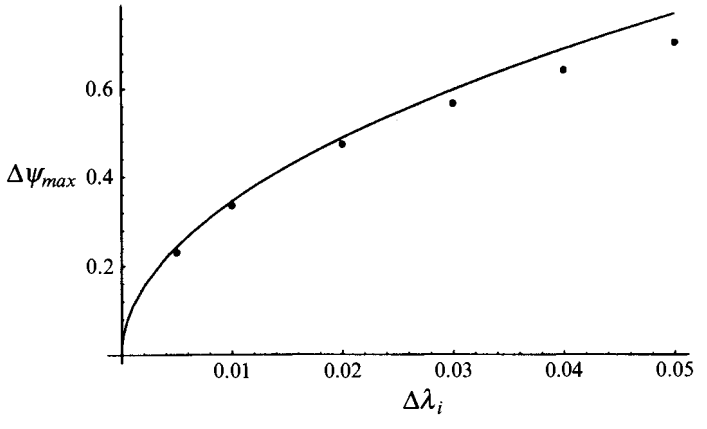

FIGURE 7. Maximum oscillating amplitude $\Delta\psi_{max}$ (on top of the stationary amplitudes of the original soliton) in the vicinity of the marginal stable point $\lambda_i = -0.295$, $\delta = 0.36$. Solid line from theory and dots from numerical simulation. We move into region II keeping δ fixed.

dimensional dynamical systems we can confirm that here a generic route to temporal chaos appears with spatially coherent nonlinear structures.

Note that space–time plots of $\psi(x,t)$, e.g. $\mathrm{Re}\,\psi(x,t)$ in figure 10 for the period-2 and time-chaotic solutions do not exhibit big differences. The reason is that the same spatially coherent mode still mainly takes part in the nonlinear dynamics.

However, when we deviate too much from the regime of marginal stability (i.e. the border between regions I and II) it may happen that the time-dependent solitary structure ultimately disappears, and, instead, the trivial solution becomes an attractor. Note that in region II the trivial solution is stable as has been shown previously.

At this stage three remarks are appropriate. First, cases of coherent modes in the chaotic dynamics of an infinite-dimensional system were first shown, although in a completely different context, by Nozaki & Bekki (1983), Yamada & Nozaki (1989), and Spatschek *et al.* (1990), Spatschek (1994). Secondly, Umeki (1991) reported,

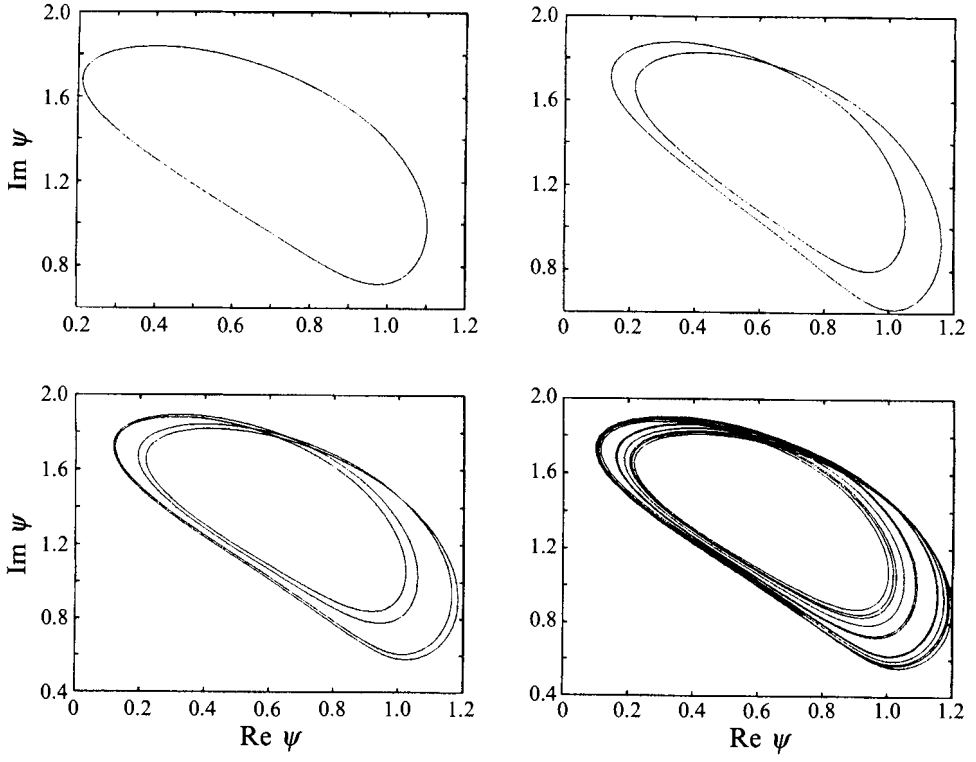

FIGURE 8. Reduced phase-space portraits $\mathrm{Im}\,\psi$ *vs.* $\mathrm{Re}\,\psi$ (we have chosen position $x = 0$, but the results are the same for any other x value) for $\delta = 0.3$ and (*a*) $\lambda_i = -0.222$, (*b*) $\lambda_i = -0.217$, (*c*) $\lambda_i = -0.214667$, and (*d*) $\lambda_i = -0.213$, respectively.

for periodic boundary conditions on a short length, a quasi-periodic route to chaos. The difference, compared to the period-doubling route to chaos presented here for long systems, is quite typical as can be understood from the analysis of Grauer & Birnir (1992). Finally, attempts to mimic this analytical behaviour by a simple collective coordinates approach are not very satisfactory here since they are not in quantitative agreement with numerical predictions. However the accuracy of this statement depends on the effort to include the relevant modes. There is no doubt that correct inclusions of the radiation mode or a model based on the most important Karhunen–Loevé modes will increase the usefulness of low-dimensional descriptions (by ordinary differential equations), but this is beyond the scope of this paper.

3.3. *The paths II → IV and III → IV*

We have seen that paths I → III lead to a bifurcation in space, whereas the transition I → II lead to a generic route in time. The two borderlines, as depicted in figure 4 follow from the papers of Laedke & Spatschek (1991) and Barashenkov *et al.* (1991), respectively. However, as shown in figure 4, there is an overlapping region IV. First of all, when we start with a noidal wave solution of region III and move to IV period-doubling bifurcations can also be seen. These types of paths have been extensively investigated by Umeki (1991 *a*). Therefore, there is no need to present them here again. We should mention that we have confirmed his simulations for relatively small distances L and obtained behaviour similar to the solitary case for larger systems.

Here we would like to show only one typical example for relatively long distances

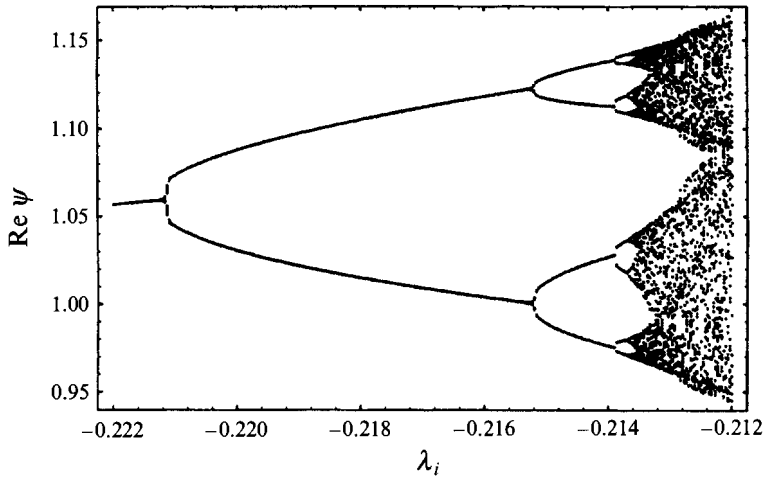

FIGURE 9. Sequence of period-dodoubling bifurcations for $\delta = 0.3$.

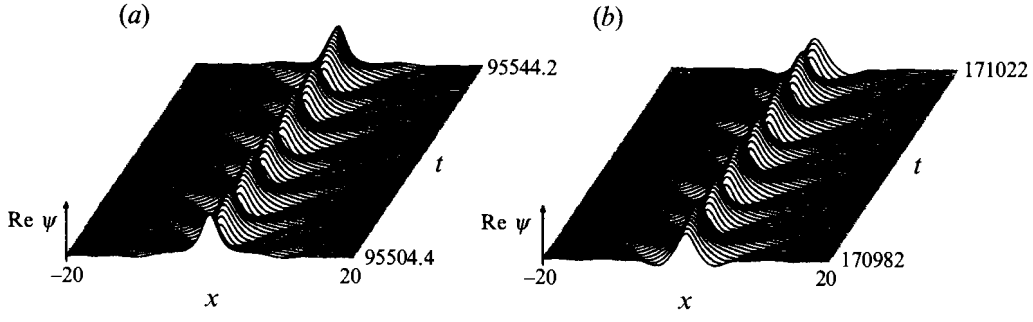

FIGURE 10. Space–time plots of Re ψ for $\delta = 0.3$ and (*a*) $\lambda_i = -0.217$ and (*b*) $\lambda_i = -0.213$, respectively.

($L = 40$) which we computed by moving deep into the region IV. Time- and space-chaotic solutions can appear as is shown in figure 11.

In contrast to the previous case, however, in IV the trivial solution is unstable so that it cannot appear as an attractor.

4. Non-propagating soliton under a periodically modulated oscillation

Recently the problem was considered of when the tank is subjected vertically to a periodically amplitude-modulated harmonic oscillation instead of a pure simple harmonic oscillation (Chen & Wei 1994). Such investigations are very interesting since they throw some light onto the importance of soliton modes in nonlinear dynamics of infinite-dimensional non-integrable systems (Spatschek 1994). In the present formulation it means that we allow for $a_m \neq 0$. The basic experimental findings from a Plexiglas rectangular tank filled with water were reported by Chen & Wei (1994), who also presented numerical simulations and a simple theoretical model. Our numerical code can easily reproduce the numerical simulations; a typical picture of a modulated soliton is shown in figure 12.

We would like to emphasize one point. The stable existence region of an un-

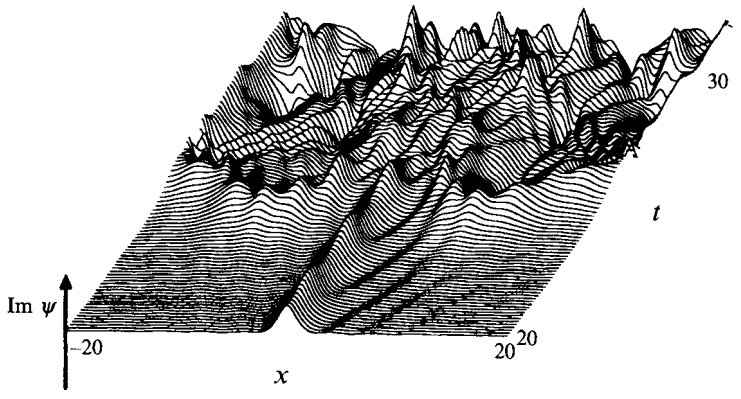

FIGURE 11. A space- and time-chaotic solution for $\mathrm{Im}\,\psi$ appears, e.g., at $\delta = 1.1652$ and $\lambda_i = -0.1584$.

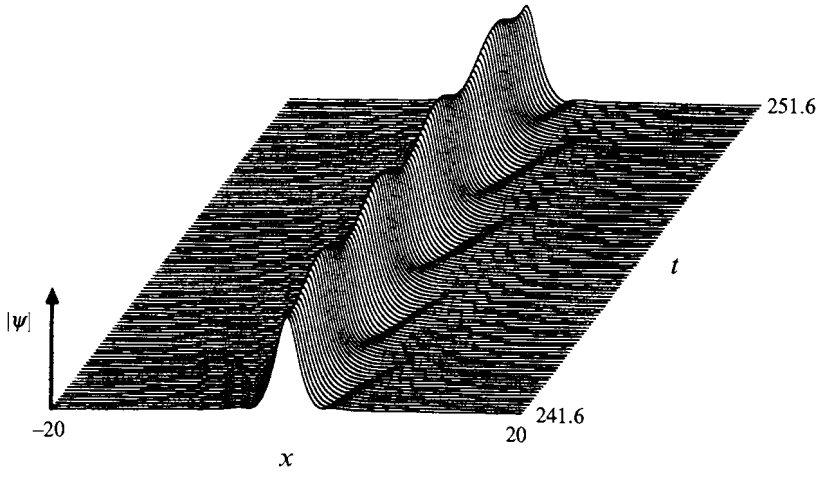

FIGURE 12. Space–time plot of a non-propagating soliton under a periodically modulated oscillation. The parameter values are $\delta = 0.75$, $\lambda_i = -0.6$, $\lambda_r = +1$, $\Omega = 2.6$, and $a_m = 0.2$.

modulated soliton is shown in figure 4 as region I. By modulation a frequency Ω appears which in general is incommensurable with the frequency ω_1 observed in the Hopf bifurcation I $\rightarrow$ II. Thus in II we get a quasi-periodic solution in time as shown in figure 12. With respect to period $2\pi/\Omega$ a period-doubling route to chaos can occur when we increase the modulated amplitude a_m. (Note that this appears in addition to the period-doubling route to chaos along I $\rightarrow$ II for decreasing $-\lambda_i$ and $a_m \equiv 0$.) Thus the numerical situation is quite clear.

However, when aiming for analytical low-dimensional reduced models one should be careful with quantitative predictions. The reason is that in the unperturbed (i.e. not modulated) state we should really start with a soliton in region I, and all the previous investigations (e.g. Nozaki & Bekki 1983) showed that the inclusion of the radiation mode is necessary for good quantitative agreement with experiments. It seems to us that the analytical model presented by Chen & Wei (1994) is useful for qualitative interpretations but for rigorous theoretical (quantitative) predictions the soliton mode is not sufficient in any perturbation theory. We have confirmed this suspicion by

finding clear quantitative discrepancies between the analytical predictions of Chen & Wei (1994) and the exact numerical solutions. But we believe that this quantitative aspect is not too important since one knows from other examples how to cure such a deficiency.

5. Summary and outlook

In this paper we wanted to contribute towards the general understanding of the nonlinear dynamics of non-propagating surface waves in Faraday resonance. We tried to embed our contributions into the recent literature in this field. New findings are the general non-existence theorem (§ 2.1), the nonlinear theory for the oscillating instability (§ 3.2 and the Appendix), and the prediction of a period-doubling route to chaos for long systems (§ 3.2) in contrast to the quasi-periodic route for narrow systems (Umeki 1991*a*). Next we shall try to derive a nonlinear theory of the transition I $\rightarrow$ III, i.e. the bifurcation in space. All our calculations are strictly valid only in the finite-but-small amplitude limit. The fascinating aspect is, however, the robustness of the localized states, which leads us to expect that the conclusions are even true beyond the small-amplitude limit.

The analytical and numerical methods developed here have been worked out for applications in the Sonderforschungsbereich 191. The support of the Deutsche Forschungsgemeinschaft is gratefully acknowledged. Parts of this work belong to the thesis of one of the authors (H. F.). Discussions with members of the European project SC*–CT91–0705 are also gratefully acknowledged.

Appendix. Ginzburg–Landau model at the transition I $\rightarrow$ II

Let us introduce the notation

$$\Psi = (G + a + \mathrm{i}b)\,\mathrm{e}^{\mathrm{i}\varphi} \tag{A 1}$$

where $G\mathrm{e}^{\mathrm{i}\varphi}$ is the stationary solitary wave solution ($G = s_+$). Introducing this ansatz into the dynamical equation for ψ, we obtain with $\zeta := -\delta\cos(2\varphi)$ the coupled equations

$$a_t = -b_{xx} - G^2 b + \eta^2 b - 2\zeta b - 2Gab - (a^2 + b^2)b\,, \tag{A 2}$$

$$b_t = a_{xx} + 3G^2 a - \eta^2 a + 2\lambda_i b + G(3a^2 + b^2) + (a^2 + b^2)a\,, \tag{A 3}$$

which can be also written in the form

$$a_t = Hb - 2Gab - (a^2 + b^2)b\,, \tag{A 4}$$

$$b_t = -H_- a + 2\lambda_i b + G(3a^2 + b^2) + (a^2 + b^2)a\,, \tag{A 5}$$

defining the generators H and H_-.

Without loss of generality we can write the perturbations in the form

$$a(x,t) = \sum_{n=-\infty}^{\infty} a_n(x,t)\mathrm{e}^{\mathrm{i}n\omega t} \quad \text{with} \quad a_{-n} = a_n^*\,, \tag{A 6}$$

$$b(x,t) = \sum_{n=-\infty}^{\infty} b_n(x,t)\mathrm{e}^{\mathrm{i}n\omega t} \quad \text{with} \quad b_{-n} = b_n^*\,. \tag{A 7}$$

Let us discuss now the region close to the onset of instability at the borderline of regions I and II. We have a marginal mode with (real) frequency ω_0. The amplitude of the first harmonic will be dominating, i.e. it will be of first order in the smallness parameter ω. In addition, we shall have the nearest-neighbour harmonics, as well as a weak time-dependence of the amplitudes. This suggests the ansatz

$$a_0(x,t) = \epsilon^2 a_{02}(\epsilon^2 t, x, \epsilon x, \epsilon^2 x) + \epsilon^3 a_{03} + \cdots , \tag{A 8}$$

$$b_0(x,t) = \epsilon^2 b_{02}(\epsilon^2 t, x, \epsilon x, \epsilon^2 x) + \epsilon^3 b_{03} + \cdots \tag{A 9}$$

for $n = 0$,

$$a_2(x,t) = \epsilon^2 a_{22}(\epsilon^2 t, x, \epsilon x, \epsilon^2 x) + \epsilon^3 a_{23} + \cdots , \tag{A 10}$$

$$b_2(x,t) = \epsilon^2 b_{22}(\epsilon^2 t, x, \epsilon x, \epsilon^2 x) + \epsilon^3 b_{23} + \cdots \tag{A 11}$$

for $n = 2$ and

$$a_1(x,t) = \epsilon A(\epsilon^2 t, \epsilon x, \epsilon^2 x)\hat{a} + \epsilon^2 a_{12} + \epsilon^3 a_{13} + \cdots , \tag{A 12}$$

$$b_1(x,t) = \epsilon A(\epsilon^2 t, \epsilon x, \epsilon^2 x)\hat{b} + \epsilon^2 b_{12} + \epsilon^3 b_{13} + \cdots \tag{A 13}$$

for $n = 1$.

Here, ϵ is the smallness parameter, and $\hat{a}$ and $\hat{b}$ are the amplitudes of the marginal modes after separating $e^{i\omega_0 t}$, i.e.

$$i\omega_0 \hat{a} - H_0 \hat{b} = 0 , \tag{A 14}$$

$$H_- \hat{a} + (i\omega_0 - 2\lambda_{i0})\hat{b} = 0 \tag{A 15}$$

within a linear approximation. The definitions of the operators follow by comparing with the corresponding explicit equations, e.g. we also define

$$H_0 := H_+ - 2\zeta_0 , \tag{A 16}$$

$$\boldsymbol{T}_n := \begin{pmatrix} in\omega_0 & -H_0 \\ H_- & in\omega_0 - 2\lambda_{i0} \end{pmatrix} . \tag{A 17}$$

Note that the index 0 always characterizes the quantities exactly at the marginal point. For the marginal mode we have

$$\boldsymbol{T}_1 \begin{pmatrix} \hat{a} \\ \hat{b} \end{pmatrix} = 0 . \tag{A 18}$$

In the neigbourhood of a marginal point ζ_0 and λ_{i0} we expand

$$\lambda_i = \lambda_{i0} + \epsilon^2 \lambda_{i2} + \cdots , \tag{A 19}$$

$$\zeta = \zeta_0 + \epsilon^2 \zeta_2 + \cdots , \tag{A 20}$$

and use

$$t_2 := \epsilon^2 t , \quad x_0 := x , \quad x_1 := \epsilon x , \quad x_2 := \epsilon^2 x \tag{A 21}$$

with $\omega = \omega_0$. Next, we need the kernel of the adjoint operator

$$\boldsymbol{T}_1^\dagger = \begin{pmatrix} -i\omega_0 & H_- \\ -H_0 & -i\omega_0 - 2\lambda_{i0} \end{pmatrix} ; \tag{A 22}$$

for that we introduce

$$\begin{pmatrix} \tilde{a} \\ \tilde{b} \end{pmatrix} := \begin{pmatrix} H_- \hat{a}^* \\ -H_0 \hat{b}^* \end{pmatrix} . \tag{A 23}$$

Then

$$\boldsymbol{T}_1^{\dagger}\begin{pmatrix}\tilde{a}\\ \tilde{b}\end{pmatrix}=\begin{pmatrix}-\mathrm{i}\omega_0 H_- & -H_- H_0\\ -H_0 H_- & (\mathrm{i}\omega_0+2\lambda_{i0})H_0\end{pmatrix}\begin{pmatrix}\hat{a}^*\\ \hat{b}^*\end{pmatrix}$$
$$=\begin{pmatrix}H_- & 0\\ 0 & H_0\end{pmatrix}\boldsymbol{T}_1^*\begin{pmatrix}\hat{a}^*\\ \hat{b}^*\end{pmatrix}$$
$$=\begin{pmatrix}H_- & 0\\ 0 & H_0\end{pmatrix}\left[\boldsymbol{T}_1\begin{pmatrix}\hat{a}\\ \hat{b}\end{pmatrix}\right]^*=0\,. \tag{A 24}$$

From here we conclude that (A 23) leads directly to the kernel $\tilde{a}$ and $\tilde{b}$ of $\boldsymbol{T}_1^{\dagger}$.

Now we introduce the ansatzes into the basic equations and collect orders in ϵ. The first order in ϵ yields for $n=1$

$$A\boldsymbol{T}_1\begin{pmatrix}\hat{a}\\ \hat{b}\end{pmatrix}=0\,. \tag{A 25}$$

Order ϵ^2 and $n=0$ follows from

$$\boldsymbol{T}_0\begin{pmatrix}a_{02}\\ b_{02}\end{pmatrix}=2G\begin{pmatrix}-\hat{a}^*\hat{b}-\hat{a}\hat{b}^*\\ 3|\hat{a}|^2+|\hat{b}|^2\end{pmatrix}|A|^2\,, \tag{A 26}$$

with the result

$$\begin{pmatrix}a_{02}\\ b_{02}\end{pmatrix}=2|A|^2\boldsymbol{T}_0^{-1}\begin{pmatrix}-(\hat{a}^*\hat{b}+\hat{a}\hat{b}^*)G\\ (3|\hat{a}|^2+|\hat{b}|^2)G\end{pmatrix}. \tag{A 27}$$

Using

$$\begin{pmatrix}\tilde{a}_{02}\\ \tilde{b}_{02}\end{pmatrix}:=2\boldsymbol{T}_0^{-1}\begin{pmatrix}-(\hat{a}^*\hat{b}+\hat{a}\hat{b}^*)G\\ (3|\hat{a}|^2+|\hat{b}|^2)G\end{pmatrix} \tag{A 28}$$

we have

$$\begin{pmatrix}a_{02}\\ b_{02}\end{pmatrix}=|A|^2\begin{pmatrix}\tilde{a}_{02}\\ \tilde{b}_{02}\end{pmatrix}. \tag{A 29}$$

For $n=1$ and second order in ϵ we obtain

$$\boldsymbol{T}_1\begin{pmatrix}a_{12}\\ b_{12}\end{pmatrix}=2\frac{\partial A}{\partial x_1}\frac{\partial}{\partial x_0}\begin{pmatrix}-\hat{b}\\ \hat{a}\end{pmatrix}. \tag{A 30}$$

Since

$$\boldsymbol{T}_1\begin{pmatrix}x_0\hat{a}\\ x_0\hat{b}\end{pmatrix}=-2\frac{\partial}{\partial x_0}\begin{pmatrix}-\hat{b}\\ \hat{a}\end{pmatrix}, \tag{A 31}$$

we can define

$$\begin{pmatrix}\tilde{a}_{12}\\ \tilde{b}_{12}\end{pmatrix}:=-\begin{pmatrix}x_0\hat{a}\\ x_0\hat{b}\end{pmatrix} \tag{A 32}$$

such that

$$\begin{pmatrix}a_{12}\\ b_{12}\end{pmatrix}=\frac{\partial A}{\partial x_1}\begin{pmatrix}\tilde{a}_{12}\\ \tilde{b}_{12}\end{pmatrix} \tag{A 33}$$

can be solved. For $n=2$ we have

$$\boldsymbol{T}_2\begin{pmatrix}a_{22}\\ b_{22}\end{pmatrix}=G\begin{pmatrix}-2\hat{a}\hat{b}\\ 3\hat{a}^2+\hat{b}^2\end{pmatrix}A^2\,. \tag{A 34}$$

Defining

$$\begin{pmatrix} \tilde{a}_{22} \\ \tilde{b}_{22} \end{pmatrix} := \boldsymbol{T}_2^{-1} \begin{pmatrix} -2\hat{a}\hat{b}G \\ (3\hat{a}^2 + \hat{b})G \end{pmatrix} \tag{A 35}$$

we finally obtain

$$\begin{pmatrix} a_{22} \\ b_{22} \end{pmatrix} = A^2 \begin{pmatrix} \tilde{a}_{22} \\ \tilde{b}_{22} \end{pmatrix} . \tag{A 36}$$

$\boldsymbol{T}_2$ can be inverted since H_- and H_0 are self-adjoint.

Now the more complicated but most interesting order ϵ^3:

$$\begin{aligned} \boldsymbol{T}_1 \begin{pmatrix} a_{13} \\ b_{13} \end{pmatrix} = & -\frac{\partial A}{\partial t_2} \begin{pmatrix} \hat{a} \\ \hat{b} \end{pmatrix} + 2\frac{\partial A}{\partial x_2}\frac{\partial}{\partial x_0} \begin{pmatrix} -\hat{b} \\ \hat{a} \end{pmatrix} + \frac{\partial^2 A}{\partial x_1^2} \begin{pmatrix} -\hat{b} \\ \hat{a} \end{pmatrix} \\ & + 2A \begin{pmatrix} -\zeta_2 \hat{b} \\ \lambda_{i2}\hat{b} \end{pmatrix} + 2AG \begin{pmatrix} -a_{02}\hat{b} - b_{02}\hat{a} \\ 3a_{02}\hat{a} + b_{02}\hat{b} \end{pmatrix} \\ & + 2A^* G \begin{pmatrix} -b_{22}\hat{a}^* - a_{22}\hat{b}^* \\ 3a_{22}\hat{a}^* + b_{22}\hat{b}^* \end{pmatrix} + 2\frac{\partial}{\partial x_1}\frac{\partial}{\partial x_0} \begin{pmatrix} -b_{12} \\ a_{12} \end{pmatrix} \\ & + |A|^2 A \begin{pmatrix} -2\hat{b}|\hat{a}|^2 - \hat{a}^2\hat{b}^* - 3\hat{b}|\hat{b}|^2 \\ 2\hat{a}|\hat{b}|^2 + \hat{b}^2\hat{a}^* + 3\hat{a}|\hat{a}|^2 \end{pmatrix} . \end{aligned} \tag{A 37}$$

This can be written as

$$\begin{aligned} \boldsymbol{T}_1 \begin{pmatrix} a_{13} \\ b_{13} \end{pmatrix} = & -\frac{\partial A}{\partial t_2} \begin{pmatrix} \hat{a} \\ \hat{b} \end{pmatrix} + 2\frac{\partial A}{\partial x_2}\frac{\partial}{\partial x_0} \begin{pmatrix} -\hat{b} \\ \hat{a} \end{pmatrix} + \frac{\partial^2 A}{\partial x_1^2} \begin{pmatrix} -\hat{b} \\ \hat{a} \end{pmatrix} \\ & + 2A \begin{pmatrix} -\zeta_2 \hat{b} \\ \lambda_{i2}\hat{b} \end{pmatrix} + 2|A|^2 AG \begin{pmatrix} -\tilde{a}_{02}\hat{b} - \tilde{b}_{02}\hat{a} \\ 3\tilde{a}_{02}\hat{a} + \tilde{b}_{02}\hat{b} \end{pmatrix} \\ & + 2|A|^2 AG \begin{pmatrix} -\tilde{b}_{22}\hat{a}^* - \tilde{a}_{22}\hat{b}^* \\ 3\tilde{a}_{22}\hat{a}^* + \tilde{b}_{22}\hat{b}^* \end{pmatrix} + 2\frac{\partial^2 A}{\partial x_1^2}\frac{\partial}{\partial x_0} \begin{pmatrix} -\tilde{b}_{12} \\ \tilde{a}_{12} \end{pmatrix} \\ & + |A|^2 A \begin{pmatrix} -2\hat{b}|\hat{a}|^2 - \hat{a}^2\hat{b}^* - 3\hat{b}|\hat{b}|^2 \\ 2\hat{a}|\hat{b}|^2 + \hat{b}^2\hat{a}^* + 3\hat{a}|\hat{a}|^2 \end{pmatrix} . \end{aligned} \tag{A 38}$$

Equation (A 38) requires a solvability condition. Multiplying from the left with the kernel of $\boldsymbol{T}_1^\dagger$ and integrating leads to

$$\begin{aligned} 0 = & -\left\langle \begin{pmatrix} \tilde{a} \\ \tilde{b} \end{pmatrix} \middle| \begin{pmatrix} \hat{a} \\ \hat{b} \end{pmatrix} \right\rangle \frac{\partial A}{\partial t_2} + \left\langle \begin{pmatrix} \tilde{a} \\ \tilde{b} \end{pmatrix} \middle| \begin{pmatrix} -\hat{b} \\ \hat{a} \end{pmatrix} \right\rangle \frac{\partial^2 A}{\partial x_1^2} \\ & + \left\langle \begin{pmatrix} \tilde{a} \\ \tilde{b} \end{pmatrix} \middle| \begin{pmatrix} -2\zeta_2 \hat{b} \\ 2\lambda_{i2}\hat{b} \end{pmatrix} \right\rangle A + \left\langle \begin{pmatrix} \tilde{a} \\ \tilde{b} \end{pmatrix} \middle| \begin{pmatrix} -\frac{\partial \tilde{b}_{12}}{\partial x_0} \\ \frac{\partial \tilde{a}_{12}}{\partial x_0} \end{pmatrix} \right\rangle \frac{\partial^2 A}{\partial x_1^2} \\ & + \left\langle \begin{pmatrix} \tilde{a} \\ \tilde{b} \end{pmatrix} \middle| \begin{pmatrix} -2(\tilde{a}_{02}\hat{b} + \tilde{b}_{02}\hat{a})G \\ 2(3\tilde{a}_{02}\hat{a} + \tilde{b}_{02}\hat{b})G \end{pmatrix} \right\rangle |A|^2 A \\ & + \left\langle \begin{pmatrix} \tilde{a} \\ \tilde{b} \end{pmatrix} \middle| \begin{pmatrix} -2(\tilde{b}_{22}\hat{a}^* + \tilde{a}_{22}\hat{b}^*)G \\ 2(3\tilde{a}_{22}\hat{a}^* + \tilde{b}_{22}\hat{b}^*)G \end{pmatrix} \right\rangle |A|^2 A \\ & + \left\langle \begin{pmatrix} \tilde{a} \\ \tilde{b} \end{pmatrix} \middle| \begin{pmatrix} -2\hat{b}|\hat{a}|^2 - \hat{a}^2\hat{b}^* - 3\hat{b}|\hat{b}|^2 \\ 2\hat{a}|\hat{b}|^2 + \hat{b}^2\hat{a}^* + 3\hat{a}|\hat{a}|^2 \end{pmatrix} \right\rangle |A|^2 A . \end{aligned} \tag{A 39}$$

Now using the definitions

$$N := \left\langle \begin{pmatrix} \tilde{a} \\ \tilde{b} \end{pmatrix} \middle| \begin{pmatrix} \hat{a} \\ \hat{b} \end{pmatrix} \right\rangle , \tag{A 40}$$

$$\alpha := \frac{1}{N} \left\langle \begin{pmatrix} \tilde{a} \\ \tilde{b} \end{pmatrix} \middle| \begin{pmatrix} -2\zeta_2 \hat{b} \\ 2\lambda_{i2} \hat{b} \end{pmatrix} \right\rangle , \tag{A 41}$$

$$\beta := 0 , \tag{A 42}$$

$$\begin{aligned} \gamma := \frac{1}{N} \Bigg\{ & \left\langle \begin{pmatrix} \tilde{a} \\ \tilde{b} \end{pmatrix} \middle| \begin{pmatrix} -2(\tilde{a}_{02}\hat{b} + \tilde{b}_{02}\hat{a})G \\ 2(3\tilde{a}_{02}\hat{a} + \tilde{b}_{02}\hat{b})G \end{pmatrix} \right\rangle \\ & + \left\langle \begin{pmatrix} \tilde{a} \\ \tilde{b} \end{pmatrix} \middle| \begin{pmatrix} -2(\tilde{b}_{22}\hat{a}^* + \tilde{a}_{22}\hat{b}^*)G \\ 2(3\tilde{a}_{22}\hat{a}^* + \tilde{b}_{22}\hat{b}^*)G \end{pmatrix} \right\rangle \\ & + \left\langle \begin{pmatrix} \tilde{a} \\ \tilde{b} \end{pmatrix} \middle| \begin{pmatrix} -2\hat{b}|\hat{a}|^2 - \hat{a}^2\hat{b}^* - 3\hat{b}|\hat{b}|^2 \\ 2\hat{a}|\hat{b}|^2 + \hat{b}^2\hat{a}^* + 3\hat{a}|\hat{a}|^2 \end{pmatrix} \right\rangle \Bigg\} \end{aligned} \tag{A 43}$$

we have derived a complex Ginzburg–Landau equation

$$A_{t_2} = \alpha A + \beta A_{x_1 x_1} + \gamma |A|^2 A . \tag{A 44}$$

REFERENCES

Barashenkov, I. V., Bogdan, M. M. & Korobov, V. I. 1991 Stability diagram of the phase-locked solitons in the parametrically driven, damped nonlinear Schrödinger equation. *Europhys. Lett.* **15**, 113–118.

Chen, X.-N. & Wei, R.-J. 1994 Dynamic behaviour of a non-propagating soliton under a periodically modulated oscillation. *J. Fluid Mech.* **259**, 291–303.

Ciliberto, S. & Gollub, J. P. 1985 Chaotic mode competition in parametrically forced surface waves. *J. Fluid Mech.* **158**, 391–398.

Denardo, B., Wright, W., Putterman, S. & Larraza, A. 1990 Observation of a kink soliton on the surface of a liquid. *Phys. Rev. Lett.* **64**, 1518–1521.

Ezerskii, A. B., Rabinovich, M. I., Rentov, V. P. & Starobinets, M. 1986 Spatiotemporal chaos in the parametric excitation of a capillary ripple. *Sov. Phys. JETP* **64**, 1228–1236.

Funakoshi, M. & Inoue, S. 1987 Surface waves due to resonant horizontal oscillation. *J. Fluid Mech.* **192**, 219–247.

Funakoshi, M. & Inoue, S. 1990 Bifurcations of limit cycles in surface waves due to resonant forcing. *Fluid Dyn. Res.* **5**, 225–271.

Funakoshi, M. & Inoue, S. 1992 Stable periodic orbits of equations for resonantly forced water waves. *J. Phys. Soc. Japan* **61**, 3411–3412.

Grauer, R. & Birnir, B. 1992 The center manifold and bifurcations of damped and driven sine-Gordon breathers. *Physica* D **56**, 165–184.

Guthart, G. S. & Wu, T. Y.-T. 1991 Observation of a standing kink cross wave parametrically excited. *Proc. R. Soc. Lond.* A **434**, 435–440.

Kambe, J. & Umeki, M. 1990 Nonlinear dynamics of two-mode interactions in parametric excitation of surface waves. *J. Fluid Mech.* **212**, 373–393.

Laedke, E. W. & Spatschek, K. H. 1991 On localized solutions in nonlinear Faraday resonance. *J. Fluid Mech.* **223**, 589–601.

Larraza, A. & Putterman, S. 1984 Theory of non-propagating surface-wave solitons. *J. Fluid Mech.* **148**, 443–449.

Miles, J. W. 1984*a* Nonlinear Farady resonance. *J. Fluid Mech.* **146**, 285–302.

Miles, J. W. 1984*b* Parametrically excited solitary waves. *J. Fluid Mech.* **148**, 451–460.

Miles, J. W. 1994 A note on slowly modulated Faraday waves (preprint).

MILES, J. W. & HENDERSON, D. 1990 Parametrically forced surface waves. *Ann. Rev. Fluid Mech.* **22**, 143–165.

NEWELL, A. C. & WHITEHEAD, J. A. 1969 Finite bandwidth, finite amplitude convection. *J. Fluid Mech.* **38**, 279–303.

NOZAKI, K. & BEKKI, N. 1983 Chaos in a perturbed nonlinear Schrödinger equation. *Phys. Rev. Lett.* **50**, 1226–1229.

SASAKI, K. 1993 Standing-wave solitons on an interface between layered fluids in a channel. *J. Phys. Soc. Japan* **62**, 2675–2684.

SIMONELLI, F. & GOLLUB, J. P. 1989 Surface mode interactions: effects of symmetry and degeneracy. *J. Fluid Mech.* **199**, 471–494.

SPATSCHEK, K. H. 1994 Soliton systems in the presence of amplification, irregularities, and damping. In *Nonlinear coherent structures in physics and biology* (ed. K. H. Spatschek & F. G. Mertens). Plenum, in press.

SPATSCHEK, K.H., PIETSCH, H., LAEDKE, E.W. & EICKERMANN, TH. 1990 Chaotic behaviour in time in nonlinear Schrödinger systems. In *Nonlinear World, Vol. 2* (ed. V. G. Baryakhtar *et al.*), pp. 978–1001. World Scientific.

UMEKI, M. 1991*a* Parametric dissipative nonlinear Schrödinger equation. *J. Phys. Soc. Japan* **60**, 146–167.

UMEKI, M. 1991*b* Faraday resonance in rectangular geometry. *J. Fluid Mech.* **227**, 161–192.

WEI, R., WANG, B., MAO, Y., MIAO, G. & ZHENG, X. 1990 Further investigation of nonpropagating solitons and their transition to chaos. *J. Acoust. Soc. Am.* **88**, 469–472.

WU, J., KEOLIAN, R. & RUDNICK, I. 1984 Observation of non-propagating hydrodynamic soliton. *Phys. Rev. Lett.* **52**, 1421–1424.

YAMADA, T & NOZAKI, K. 1989 Effects of dissipative perturbation on bound-state solitons of nonlinear Schrödinger equation. *J. Phys. Soc. Japan* **58**, 1944–1947.